Power Management Strategy for a Parallel Hybrid Electric Truck

Chan-Chiao Lin, Huei Peng, J.W. Grizzle and Jun-Mo Kang

Abstract— **Hybrid vehicle techniques have been widely studied recently because of their potential to significantly improve the fuel economy and drivability of future ground vehicles. Due to the dual-power-source nature of these vehicles, control strategies based on engineering intuition frequently fail to fully explore the potential of these advanced vehicles. In this paper, we will present a procedure for the design of a near-optimal power management strategy. The design procedure starts by defining a cost function, such as minimizing a combination of fuel consumption and selected emission species over a driving cycle. Dynamic Programming (DP) is then utilized to find the optimal control actions including the gear-shifting sequence and the power split between the engine and motor while subject to a battery SOC-sustaining constraint. Through analysis of the behavior of DP control actions, near-optimal rules are extracted, which, unlike DP control signals, are implementable. The performance of this power management control strategy is studied by using the hybrid vehicle model HE-VESIM developed at the Automotive Research Center of the University of Michigan. A trade-off study between fuel economy and emissions was performed. It was found that significant emission reduction could be achieved at the expense of a small increase in fuel consumption.**

Index Terms— **Hybrid Electric Vehicle, Power Management Strategy, Powertrain Control.**

I. Introduction

Medium and heavy trucks running on diesel engines serve an important role in modern societies. More than 80% of the freight transported in the US in 1999 was carried by medium and heavy trucks. The increasing reliance on the trucking transportation brings with it certain negative impacts. First, the petroleum consumption used in the transportation sector was one of the leading contributors for the import oil gap. Furthermore, diesel-engine vehicles are known to be more polluting than gasoline-engine vehicles, in terms of NOx (Nitrogen Oxides) and PM (Particulate Matters) emissions. Recently, hybrid electric vehicle (HEV) technology has been proposed as the technology for new vehicle configurations. Owing to their dual on-board power sources and possibility of regenerative braking, HEVs offer unprecedented potential for higher fuel economy while meeting tightened emissions standard, particularly when a parallel configuration is employed. To fully realize the potential of hybrid powertrains, the power management function of these vehicles must be carefully designed. The term, "power management", refers to the design of the higher-level control algorithm that determines the proper power level to be generated, and its split between the two power sources. In general, the power management control is implemented in the vehicle-level control system that can coordinate the overall hybrid powertrain to satisfy certain performance target such as fuel economy and emissions reduction. Its commands then become the set-points for the servo-loop control systems, which operate at a much higher frequency. The servo-loop control systems can be designed for different goals, such as improved drivability, while ensuring the set-points commanded by the main loop controller are achieved reliably.

Power management strategies for parallel HEVs can be roughly classified into three categories. The first type employs heuristic control techniques such as control rules/fuzzy logic/neural networks for estimation and control algorithm development ([1], [2]). The second approach is based on static optimization methods. Commonly, electric power is translated into an equivalent amount of (steady-state) fuel rate in order to calculate the overall fuel cost ([3], [4]). The optimization scheme then figures out the proper split between the two energy sources using steady-state efficiency maps. Because of the simple point-wise optimization nature, it is possible to extend such optimization schemes to solve the simultaneous fuel economy and emission optimization problem [5]. The basic idea of the third type of HEV control algorithms considers the dynamic nature of the system when performing the optimization ([6], [7], [8]). Furthermore, the optimization is with respect to a time horizon, rather than for an instant in time. In general, power split algorithms resulting from dynamic optimization approaches are more accurate under transient conditions, but are computationally more intensive.

In this paper, we apply the Dynamic Programming (DP) technique to solve the optimal power management problem of a hybrid electric truck. The optimal power management solution over a driving cycle is obtained by minimizing a defined cost function. Two cases are solved: a fuel-economy-only case, and a fuel/emission case. The comparison of these two cases provides insight into the change needed when the additional objective of emission reduction is included. However, the DP control actions are not implementable due to their preview nature and heavy computational requirement. They are, on the other hand, a good design tool to analyze, assess and adjust other control strategies. We study the behaviour of the dynamic programming solution carefully, and extract implementable rules. These rules are used to improve a simple, intuition-based algorithm. It was found that the performance of the rule-based algorithm can be improved significantly, and in many cases, can be made to approach the

DP optimal results.

The paper is organized as follows: In Section 2, the hybrid electric truck model is described, followed by an explanation of the preliminary rule-based control strategy. The dynamic optimization problem and the DP procedure are introduced in Section 3. The optimal results for the fuel consumption and fuel/emissions optimization cases are given in Section 4. Section 5 describes the design of improved rule-based strategies. Finally, conclusions are presented in Section 6.

II. HEV SIMULATION MODEL (HE-VESIM)

A. *System Configuration*

The baseline vehicle studied is the International 4700 series, a 4X2 Class VI truck. For the hybrid configuration, the diesel engine was downsized from a V8 (7.3L) to a V6 (5.5L). In order to maintain the level of total peak, a 49 kW DC electric motor was selected from the database of electric motor models in ADVISOR program [18]. An 18 amp-hour advanced valve-regulated lead-acid (VRLA) battery was chosen as the energy storage system. The hybrid truck was found to be 246 kg heavier than the original truck. A schematic of the vehicle is given in Figure 1. The downsized engine is connected to the torque converter (TC), then to the transmission (Trns). The transmission and the electric motor are linked to the propeller shaft (PS), differential (D) and two driveshafts (DS). Important parameters of this vehicle are given in Table 1.

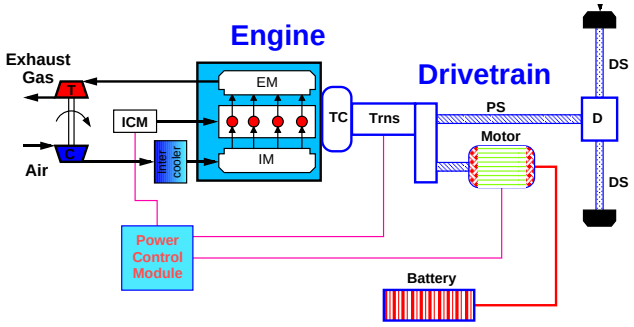

Figure 1: Schematic diagram of the hybrid electric truck

Table 1: Basic vehicle parameters

DI Diesel Engine	V6, 5.475L, 157HP/2400rpm
DC Motor	Maximum Power: 49 kW
	Maximum Torque: 274 N-m
Lead-acid Battery	Capacity: 18 Ah
	Number of modules: 25
	Nominal voltage: 12.5 (volts/module)
	Energy density: 34 (Wh/kg)
	Power density: 350 (W/kg)
Automatic Transmission	4 speed, GR: 3.45/2.24/1.41/1.0
Vehicle	Curb weight: 7504 kg

The Hybrid Engine-Vehicle SIMulation (HE-VESIM) model used in this paper is based on the conventional vehicle model VESIM developed at the University of Michigan [9]. VESIM was validated against measurements for a Class VI truck for both engine operation and vehicle launch/driving performance. The major changes from VESIM include the reduction of the engine size/power, the corresponding fuel/emission map, and the integration of the electric components. The HE-VESIM model is implemented in SIMULINK, as presented in Figure 2. For more information of the model, the reader is referred to [9] and [10].

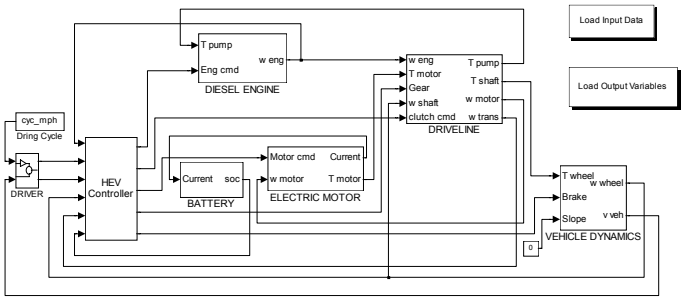

Figure 2: Vehicle model in SIMULINK

B. *Preliminary Rule Based Control Strategy*

Many existing HEV power management algorithms are rule-based, because of the ease in handling switching operating modes. For parallel hybrid vehicles, there are five possible operating modes: motor only, engine only, power-assist (engine plus motor), recharging (engine charges the battery) and, regenerative braking. In order to improve fuel economy and/or to reduce emissions, the power management controller has to decide which operating mode to use, and if proper, to determine the optimal split between the two power sources while meeting the driver's demand and maintaining battery state of charge. The simple rule-based power management strategy presented below was developed on the basis of engineering intuition and simple analysis of component efficiency tables/charts ([11], [18]), which is a very popular design approach. The design process starts by interpreting the driver pedal motion as a power request, P_{req}. According to the power request and the vehicle status, the operation of the controller is determined by one of the three control modes: Braking Control, Power Split Control and Recharging Control. If P_{req} is negative, the Braking Control is applied to decelerate the vehicle. If P_{req} is positive, either the Power Split or the Recharging Control will be applied, depending on the battery state of charge (SOC). A high-level charge-sustaining strategy tries to maintain the battery SOC within defined lower and upper bounds. A 55-60% SOC range is chosen for efficient battery operation as well as to prevent battery depletion or damage. It is important to note that these SOC levels are not hard bounds and excursions could, and commonly occur. Under normal propulsive driving conditions, the Power Split Control determines the power flow in the hybrid powertrain. When SOC drops below the lower limit, the controller will switch to the Recharging Control until the SOC reaches the upper limit, and then the Power Split Control will take over. The basic logic of each control rule is described below.

Power Split Control: Based on the engine efficiency map (Figure 3), an "engine on" power line, P_{e_on}, and "motor assist" power line, P_{m_a}, are chosen to avoid engine operation in inefficient areas. If P_{req} is less than P_{e_on}, the electric motor will supply the requested power alone. Beyond P_{e_on}, the engine becomes the sole power source. Once P_{req} exceeds P_{m_a}, engine power is set at P_{m_a} and the motor is activated to make up the difference (P_{req} - P_{m_a}).

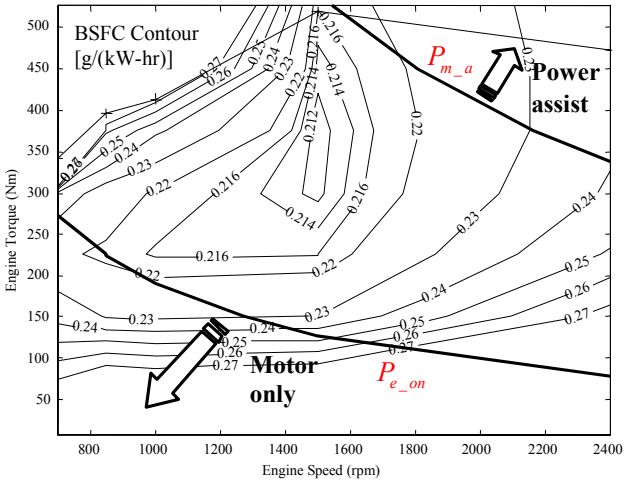

Figure 3: Power Split Control rule

Recharging Control: In the recharging control mode, the engine needs to provide additional power to charge the battery in addition to powering the vehicle. Commonly, a pre-selected recharge power level, P_{ch}, is added to the driver's power request which becomes the total requested engine power ($P_e = P_{req} + P_{ch}$). The motor power command becomes negative ($P_m = -P_{ch}$) in order to recharge the battery. One exception is that when the total requested engine power is less than P_{e_on}, the motor alone will propel the vehicle to prevent the engine from operating in the inefficient operation. In addition, when P_{req} is greater than the maximum engine power, the motor power will become positive to assist the engine.

Braking Control: A simple regenerative braking strategy is used to capture as much regenerative braking energy as possible. If P_{req} exceeds the regenerative braking capacity $P_{m\_\min}$, friction brakes will assist the deceleration ($P_b = P_{req} - P_{m\_\min}$). It should be noted that this regenerative strategy does not take the vehicle handling stability into account, which may further limit the regenerative capacity.

C. Fuel Economy and Emissions Evaluation

Unlike light-duty hybrid vehicles, heavy-duty hybrid vehicles do not yet have a standardized test procedure for measuring their emissions and fuel economy performance. A test protocol is under development by SAE and NAVC based on SAE J1711 [16] at the time we write this paper. Therefore, it was decided to follow the procedures proposed in [17]. The chassis-based driving schedule for heavy-duty vehicles (UDDSHDV), as opposed to an engine-only dynamometer cycle, is adopted. For UDDSHDV, emissions are recorded and reported in the unit of gram per mile (g/mi). In addition, the battery SOC correction procedure [17] is used to correct fuel economy and emissions in the case initial and final battery SOC are not the same. Five sets of fuel economy and emissions results can be obtained by simulating over the same driving cycle five times with different initial SOC for each run. A linear regression is then used to calculate the final fuel economy and emissions result corresponding to the zero SOC change over the cycle.

The hybrid electric truck with the preliminary rule-based controller was tested through simulation over the UDDSHDV cycle. It should be noted that because it is not straightforward to figure out whether and how the transmission should be shifted in a different manner, the shift logic of the baseline non-hybrid truck is retained in the simulation.

Table 2 compares the performance of the HEV with that of the conventional diesel engine truck. It can be seen that the hybrid-electric truck, under the preliminary rule based control algorithm, achieves 27% better fuel economy compared to the baseline diesel truck. A 10% PM reduction is also achieved even though no emission criterion is explicitly included; this is primarily due to the trickle-down effect of improved fuel economy. The NOx level increases because the engine works harder. In fact, this is exactly the main point of this paper: it is hard to include more than one objective in simple intuition-based control strategies, which are commonly driven by experience and trial-and-error. Such a simple control strategy is not optimal since it is usually component-based as oppose to system-based. Usually we do not even know how much room is left for improvement. This motivates the use of Dynamic Programming as an analysis and design tool.

Table 2: Fuel economy and engine-out emissions comparison: conventional vs. HEV

	FE (mi/gal)	NOx (g/mi)	PM (g/mi)
Conv. Truck	10.34	5.35	0.51
Hybrid Truck (Prelim. Rule-Base)	13.16	5.74	0.46

III. DYNAMIC OPTIMIZATION PROBLEM

Contrary to rule-based algorithms, the dynamic optimization approach relies on a dynamic model to compute the best control strategy. For a given driving cycle, the optimal operating strategy to minimize fuel consumption, or combined fuel consumption/emissions can be obtained. A numerical-based Dynamic Programming approach is adopted in this paper to solve this finite horizon dynamic optimization problem.

A. Problem Formulation

In the discrete-time format, a model of the hybrid electric vehicle can be expressed as:

$$x(k+1) = f(x(k), u(k)) \quad (1)$$

where $u(k)$ is the vector of control variables such as desired output torque from the engine, desired output torque from the motor, and gear shift command to the transmission. $x(k)$ is the state vector of the system. The sampling time for this main-loop control problem is selected to be one second. The optimization goal is to find the control input, $u(k)$, to minimize a cost function, which consists of the weighted sum of fuel consumption and emissions for a given driving cycle. The cost function to be minimized has the following form:

$$J = \sum_{k=0}^{N-1} L\big(x(k),u(k)\big) = \sum_{k=0}^{N-1} fuel(k) + \mu \cdot NOx(k) + \upsilon \cdot PM(k) \qquad (2)$$

where N is the duration of the driving cycle, and L is the instantaneous cost including fuel use and engine-out NOx and PM emissions. For a fuel-only problem, the weighting factors are $\mu = \upsilon = 0$. The case of $\mu > 0$ and $\upsilon > 0$ represents a simultaneous fuel/emission problem. During the optimization, it is necessary to impose the following inequality constraints to ensure safe/smooth operation of the engine/battery/motor.

$$\begin{aligned} &\omega_{e\_\min} \le \omega_e(k) \le \omega_{e\_\max} \\ &T_{e\_\min}\big(\omega_e(k)\big) \le T_e(k) \le T_{e\_\max}\big(\omega_e(k)\big) \\ &T_{m\_\min}\big(\omega_m(k), SOC(k)\big) \le T_m(k) \le T_{m\_\max}\big(\omega_m(k), SOC(k)\big) \\ &SOC_{\min} \le SOC(k) \le SOC_{\max} \end{aligned} \qquad (3)$$

where ω_e is the engine speed, T_e is the engine torque, T_m is the motor torque, SOC is the battery state of charge, and $SOC_{\min}$ and $SOC_{\max}$ are 0.4 and 0.7, respectively. In addition, we also impose two equality constraints for the optimization problem, so that the vehicle always meets the speed and load (torque) demands of the driving cycle at each sampling time.

The above problem formulation does not have any constraint on terminal SOC, the optimization algorithm tends to deplete the battery in order to attain minimal fuel consumption. Hence, a terminal constraint on SOC needs to be imposed as well:

$$\begin{aligned} J &= \sum_{k=0}^{N-1}\Big[L\big(x(k),u(k)\big)\Big] + G(x(N)) \\ &= \sum_{k=0}^{N-1}\big[fuel(k) + \mu \cdot NOx(k) + \upsilon \cdot PM(k)\big] + \alpha\big(SOC(N) - SOC_f\big)^2 \end{aligned} \qquad (4)$$

where SOC_f is the desired SOC at the final time, and α is a positive weighting factor.

B. Model Simplification

The detailed HE-VESIM model is not suitable for dynamic optimization due to its high number of states (curse of dimensionality). Thus, a simplified but sufficiently complex vehicle model is developed. Due to the fact that the system-level dynamics are the main concern of evaluating fuel economy and emissions over a long driving cycle, dynamics that are much faster than 1Hz could be ignored. By analyzing the dynamic modes, it was determined that only three state variables needed to be kept: the vehicle speed, transmission gear number, and battery SOC. The simplifications of the five sub-systems: engine, driveline, transmission, motor/battery and vehicle are described below.

1) Engine: The engine dynamics are ignored based on the quasi-static assumption [19]. The fuel consumption and engine-out emissions generated are static functions of two independent variables: engine speed and engine torque. The feed-gas NOx and PM emissions maps are obtained by scaling the emission models of a smaller diesel engine from the ADVISOR program [18]. In the current model, we assume the engine is fully warm-up; hence, engine temperature effect is not considered.

2) Driveline: The driveline components are fast and thus were reduced to static models.

$$T_p = \left(\frac{\omega_e}{K(\omega_r)}\right)^2, \qquad T_t = T_r(\omega_r)\cdot T_p \qquad (5)$$

$$T_x = \big(T_t - T_{x,l}(\omega_t, g_x)\big)\cdot R_x(g_x)\cdot \eta_x(g_x) \qquad (6)$$

$$T_d = \big(T_x + R_c \cdot T_m \cdot \eta_c - T_{d,l}(\omega_x)\big)\cdot R_d \cdot \eta_d \qquad (7)$$

where T_p and T_t are pump and turbine torques, K and T_r are the capacity factor and torque ratio of the torque converter, $\omega_r = \omega_t / \omega_e$ is the speed ratio of the torque converter, T_x and T_d are the output torque of the transmission and differential, respectively, $T_{x,l}$ and $T_{d,l}$ are the torque loss due to friction and churning loss for the transmissions and differential, respectively, R_x and η_x are gear ratio and efficiency of the transmission, which are functions of the gear number, g_x.

3) Transmission: The gear-shifting sequence of the automatic transmission is modeled as a discrete-time dynamic system with one-second time increment.

$$g_x(k+1) = \begin{cases} 4, & g_x(k) + shift(k) > 4 \\ 1, & g_x(k) + shift(k) < 1 \\ g_x(k) + shift(k), & \text{otherwise} \end{cases} \qquad (8)$$

where state, g_x, is the gear number and the control, *shift*, to the transmission is constrained to take on the values of –1, 0, and 1, representing downshift, sustain and up-shift, respectively.

4) Motor/Battery: The electric motor characteristics are based on the efficiency data obtained from [18] as shown in Figure 4. The motor efficiency is a function of motor torque and speed, $\eta_m = f(T_m, \omega_m)$. Due to the battery power and motor torque limit, the final motor torque becomes:

$$T_m = \begin{cases} \min\big(T_{m,req},\ T_{m,dis}(\omega_m),\ T_{bat,dis}(SOC,\omega_m)\big) & T_{m,req} > 0 \\ \max\big(T_{m,req},\ T_{m,chg}(\omega_m),\ T_{bat,chg}(SOC,\omega_m)\big) & T_{m,req} < 0 \end{cases} \qquad (9)$$

where $T_{m,req}$ is the requested motor torque, $T_{m,dis}$ and $T_{m,chg}$ are the maximum motor torque in the motoring and charging modes, and $T_{bat,dis}$ and $T_{bat,chg}$ are the torque bounds due to battery current limit in the discharging and charging modes.

Of all the sub-systems, the battery is perhaps the least understood. The reason for this is that the battery performance—voltage, current and efficiency as manifested from a purely electric viewpoint - is the outcome of thermally-dependent electrochemical processes that are quite complicated. If we ignore thermal-temperature effects and transients (due to internal capacitance), the battery model reduces to a static equivalent circuit shown in Figure 5. The only state variable left in the battery is the state of charge (SOC):

$$SOC(k+1) = SOC(k) - \frac{V_{oc} - \sqrt{V_{oc}^2 - 4(R_{\text{int}} + R_t)\cdot T_m \cdot \omega_m \cdot \eta_m}}{2(R_{\text{int}} + R_t)\cdot Q_b} \quad (10)$$

where the internal resistance, R_{int}, and the open circuit voltage, V_{oc}, are functions of the battery SOC, Q_b is the maximum battery charge and R_t is the terminal resistance. The battery plays an important role in the overall performance of HEVs because of its nonlinear, non-symmetric and relatively low efficiency characteristics. Figure 6 shows the charging and discharging efficiency of the battery. It can be seen that discharging efficiency decreases at low SOC and charging efficiency decreases in the high SOC region. Overall, the battery operates more efficiently at low power levels in both charging and discharging.

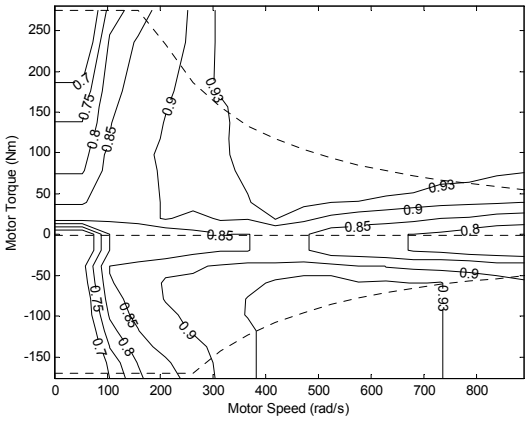

Figure 4: Efficiency map of the electric motor

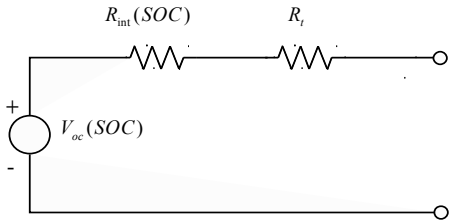

Figure 5: Static equivalent circuit battery model

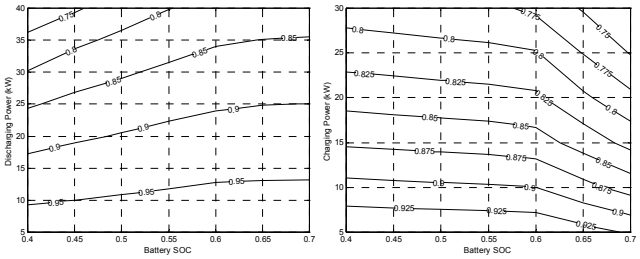

Figure 6: Energy efficiency maps of the lead acid battery: discharging (left) and charging (right).

5) Vehicle: The vehicle is modeled as a point-mass:

$$v_v(k+1) = v_v(k) + \frac{1}{M_r}\left(\frac{T_{wh}(k)}{r_d} - \frac{B_{wh}v_v(k)}{r_d^2} - \frac{v_v(k)}{|v_v(k)|}\left(F_r + F_a(v_v(k))\right)\right) \quad (11)$$

where v_v is the vehicle speed, T_{wh} is the net wheel torque from the driveline and the hydraulic brake, r_d is the dynamic tire radius, B_{wh} is the viscous damping, F_r and F_a are the rolling resistance force and the aerodynamic drag force, $M_r = M_v + J_r / r_d^2$ is the effective mass of the vehicle, and J_r is the equivalent moment of inertia of the rotating components in the vehicle. The summary of the list of symbols is listed in Table 3.

Table 3: List of symbols

Symbol	MEANING
F	force (N)
g_x	gear number
K	Torque Converter capacity factor
M	Vehicle mass (kg)
P	power (W)
R_x	gear ratio
SOC	Battery state of charge
T	torque (N-m)
v	longitudinal speed (m/s)
ω	rotational speed (rad/s)
α	weighting factor on final SOC
shift	gear shifting command
V_{oc}	open circuit voltage (V)
μ	weighting factor on NOx
υ	weighting factor on PM
η	efficiency
Subscripts	
d	differential
e	engine
l	loss
m	motor
p	pump
t	turbine
v	Vehicle
x	transmission
wh	wheel

C. Dynamic Programming Method

Dynamic programming is a powerful tool to solve general dynamic optimization problems. The main advantage is that it can easily handle the constraints and nonlinearity of the problem while obtaining a globally optimal solution [12]. The DP technique is based on Bellman's Principle of Optimality, which states that the optimal policy can be obtained if we first solve a one stage sub-problem involving only the last stage and then gradually extend to sub-problems involving the last two stages, last three stages, …etc. until the entire problem is solved. In this manner, the overall dynamic optimization problem can be decomposed into a sequence of simpler minimization problems as follows [12].

Step $N-1$:

$$J^*_{N-1}(x(N-1)) = \min_{u(N-1)}\left[L(x(N-1),u(N-1)) + G(x(N))\right] \quad (12)$$

Step k, for $0 \le k < N-1$

$$J^*_k(x(k)) = \min_{u(k)}\left[L(x(k),u(k)) + J^*_{k+1}(x(k+1))\right] \quad (13)$$

where $J^*_k(x(k))$ is the optimal cost-to-go function or optimal value function at state $x(k)$ starting from time stage *k*. It represents the optimal resulting cost that if at stage *k* the system starts at state $x(k)$ and follows the optimal control law

thereafter until the final stage.

The above recursive equation is solved backwards to find the optimal control policy. The minimizations are performed subject to the inequality constraints shown in Eq. (3) and the equality constraints imposed by the driving cycle.

D. Numerical Computation

Due to the nonlinear characteristics of the hybrid powertrain, it is not possible to solve DP analytically. Instead, DP has to be solved numerically by some approximations. A standard way to solve Eq. (13) numerically is to use quantization and interpolation ([12], [13]). For continuous state space and control space, the state and control values are first discretized into finite grids. At each step of the optimization search, the function $J_k(x(k))$ is evaluated only at the grid points of the state variables. If the next state, $x(k+1)$, does not fall exactly on a quantized value, then the values of $J^*_{k+1}(x(k+1))$ in Eq.(13) as well as $G(x(N))$ in (12) are determined through linear interpolation.

Despite the use of a simplified model and a quantized search space, the long time horizon makes the above algorithm computationally expensive. In this research, we adopted two approaches to accelerate the optimization search. First, from the speed profile of the driving cycle, the required wheel torque $T_{wh,req}$ is determined by inversely solving Eq.(11). The required wheel speed $\omega_{wh,req}$ can be computed by feeding the required wheel torque to the vehicle model in order to include the wheel dynamics and slip effect. Combining this procedure with the defined state/input grid, the vehicle model can be replaced by a finite set of operating points parameterized by $T_{wh,req}$ and $\omega_{wh,req}$. The second approach adopted is to construct pre-computed look-up tables for the new states and instantaneous cost as a function of quantized states, control inputs, and operating points. Once these tables are built, they can be used to update Eq.(13) efficiently by the vector operations in MATLAB [13].

IV. DYNAMIC PROGRAMMING RESULTS

The DP procedure described above produces an optimal, time-varying, state-feedback control law, i.e., $u^*(x(k),k)$. It should be noted that DP creates a family of optimal paths for all possible initial conditions. Once the initial SOC is specified, the optimal policy will find a way to achieve the minimal weighted cost of fuel consumption and emissions while bringing the final SOC close to the desired terminal value (SOC_f). The optimal control law was applied to the full-order HE-VESIM model for the final evaluation. In the following, two cases are presented: fuel economy only, and simultaneous fuel/emission optimization.

A. Fuel Economy Optimization Results

When optimizing for only fuel economy, the weightings μ and υ in Eq.(4) are set to zero. The UDDSHDV driving cycle is again used. The initial and terminal desired SOC were both selected to be 0.57. The weighting factor, $\alpha = 5 \cdot 10^6$, is used to assure the battery SOC will return to 0.57 at the end of the cycle. Simulation results of the vehicle under the DP policy are shown in Figure 7. There is a small difference (less than 2mph) between the desired vehicle speed (UDDSHDV) and the achieved vehicle speed, caused by model mismatch and the long sampling time (1 sec). The engine power and motor power trajectories represent the optimal operation between two power movers for achieving the best fuel economy. An additional 4% fuel economy improvement was achieved by the DP algorithm (Table 4) as compared with the value achieved by the preliminary rule-based strategy in Table 2.

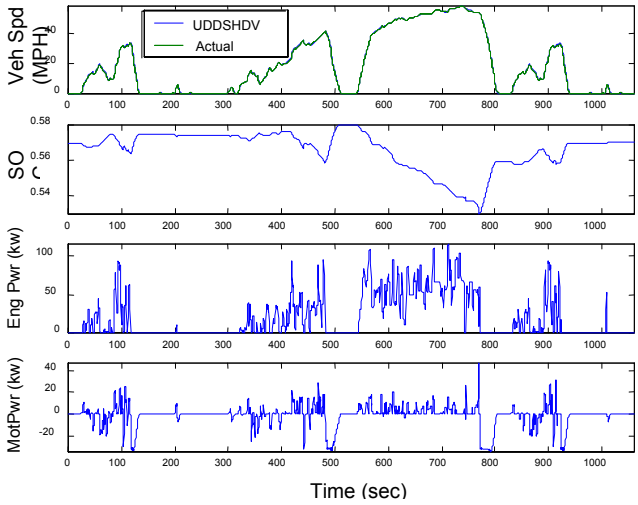

Figure 7: Simulation results for the fuel-economy-only case

Table 4: Summary of DP results for $\mu = 0, \upsilon = 0$

	FE (mi/gal)	Fuel (g/mi)	NOx (g/mi)	PM (g/mi)
$\mu = 0, \upsilon = 0$	13.71	234.71	5.63	0.45

B. Fuel Economy and Emissions Optimization

To study the trade-off between fuel economy and emissions, the weighting factors are varied:

$$\mu \in \{0, 5, 10, 20, 40\}$$
$$\upsilon \in \{0, 100, 200, 400, 600, 800, 1000\} \quad (14)$$

The relative sizes of the weighting factors are decided by comparing mean values of the look-up tables for the engine fuel rate and feedgas (NOx and PM) flow rate. The possible values for each weighting factor were chosen so that they vary in a range centered around its mean-value-inspired weighting factor to study the trade-off of the respective component for the optimization. This trade-off study is important in the early design process because it provides useful information about the sensitivity among the fuel consumption and feedgas emissions, NOx and PM. Selected optimization results are shown in Figures 8 and 9 by using the following measure to present the relative change for different weighting factors.

$$\frac{(\Phi_i)_{\mu,\upsilon} - (\Phi_i)_{\mu=\upsilon=0}}{(\Phi_i)_{\mu=\upsilon=0}} \times 100\%, \qquad i = FE,\ NOx,\ PM \quad (15)$$

where Φ_{FE}, Φ_{NOx}, and Φ_{PM} are the fuel economy, NOx

emission and PM emission over the UDDSHDV cycle, respectively. The case of $\mu=\upsilon=0$ corresponds to the fuel-economy-only scenario. Figure 8 shows the trade-off in NOx emissions and fuel economy. Increasing μ leads to significant NOx reduction while causing a small fuel economy increase. Increasing υ results in reduced PM (Figure 9) but higher NOx emissions and lower fuel economy (Figure 8). The trade-off between NOx and PM can be seen from Figure 9 where larger υ tends to decrease PM emission but increase NOx emission. More importantly, significant reduction in NOx and PM emissions can be achieved at the price of a small increase in fuel consumption.

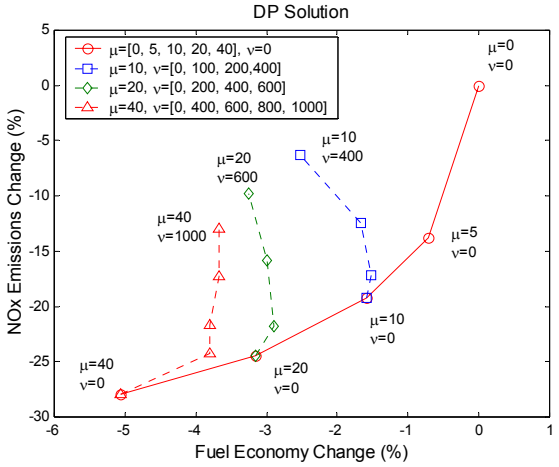

Figure 8: Fuel economy versus engine-out NOx emissions

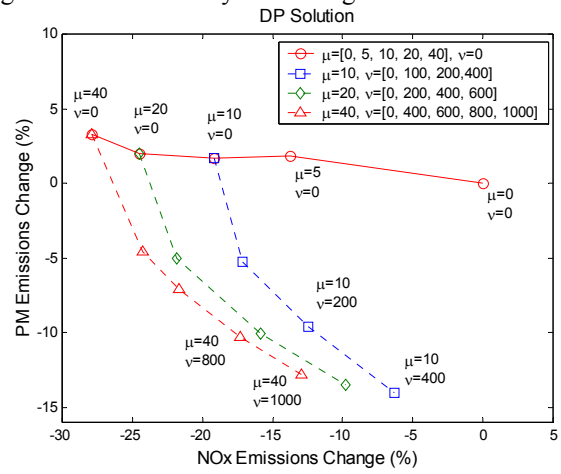

Figure 9: Engine-out PM emissions versus NOx emissions

The case with $\mu=40,\upsilon=800$ seem to achieve a good trade-off--NOx and PM are reduced by 17.3 % and 10.3% respectively at a 3.67% penalty on fuel economy. Simulation results of this case are shown in Figure 10. Battery SOC fluctuates in a wider range compared to the fuel-only case (Figure 7). It can be seen that in the case of fuel-only optimization, almost all of the negative motor power is due to regenerative braking. In other words, the engine seldom recharges the battery. Therefore, all electrical energy consumed comes from regenerative braking. This implies that it is not efficient to use engine power to charge the battery. This is due to the fact that the fuel efficiency map of this diesel engine is flat in medium to high power regions.

V. DEVELOPMENT OF IMPROVED RULE-BASED CONTROLS

The DP control policy is not implementable in real driving conditions because it requires knowledge of future speed and load profile. Nonetheless, analyzing its behavior provides useful insight into possible improvement of the rule-based controller.

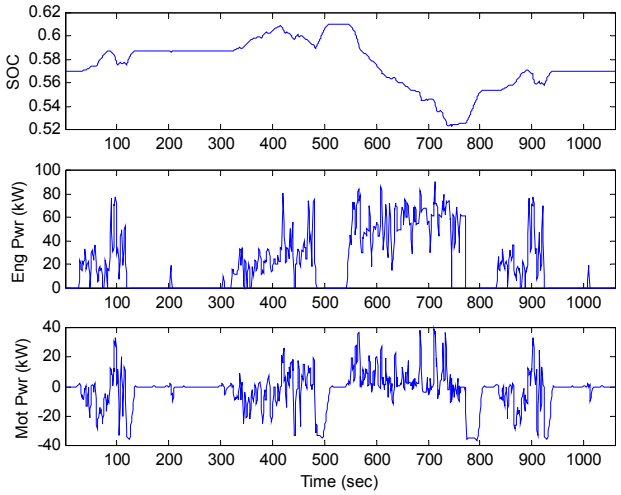

Figure 10: Simulation results ($\mu=40$ and $\upsilon=800$)

A. Gear Shift Control

The gear-shifting schedule is crucial to the fuel economy of hybrid electric vehicles [14]. In the Dynamic Programming scheme, gear-shift command is one of the control variables. It is interesting to find out how the DP solution chooses the optimal gear position to improve fuel economy and reduce emissions. It is first observed that the optimal gear trajectory has frequent shifting, which is undesirable. Hence, a drivability constraint is added to avoid this:

$$J=\sum_{k=0}^{N-1}\left(fuel(k)+40\cdot NOx(k)+800\cdot PM(k)+\beta\cdot\left|g_x(k+1)-g_x(k)\right|\right) + 5\cdot 10^6\cdot(SOC(N)-SOC_f)^2 \quad (16)$$

where β is a positive weighting factor. Figure 11 shows the optimal gear position trajectories from DP for different values of β. It can be seen that a larger value of β results in less frequent gear shifting. As a result, the optimization result of $\beta=1.5$ is used for the subsequent analysis.

From the DP results, the gear operational points are plotted on the engine power demand vs. transmission speed plot (Figure 12). It can be seen that the gear positions are separated into four regions and the boundary between adjacent regions represent optimal gear shifting thresholds. After adding a hysteresis function to the shifting thresholds, a new gear shift map is obtained. It should be mentioned that the optimal gear shift map can also be constructed through static optimization ([11], [15]). Given an engine power and wheel speed, the best gear position for minimum weighted cost of

fuel and emissions can be chosen based on the combined steady-state engine fuel consumption and emissions map. It is found that the steady-state gear map from this method nearly coincides with Figure 12.

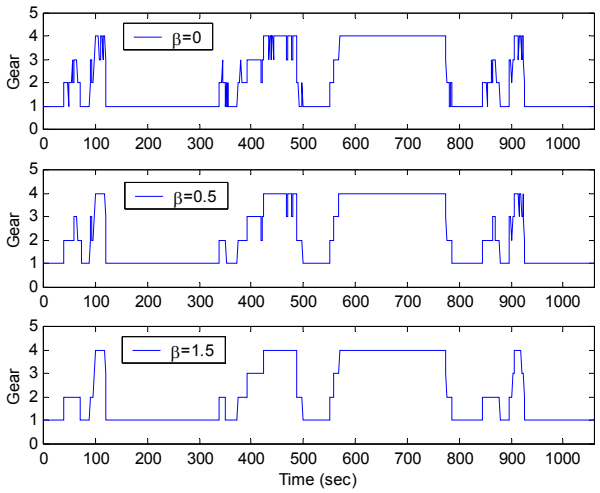

Figure 11: Optimal gear position trajectory

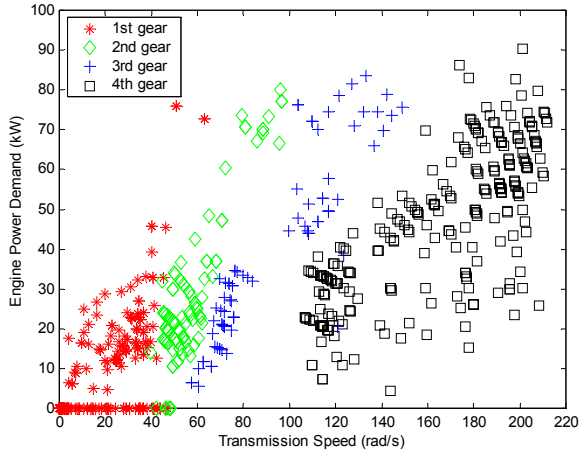

Figure 12: Gear operating points of DP optimisation

B. *Power Split Control*

In this section, we study how Power Split Control of the preliminary rule-based algorithm can be improved. A power-split-ratio $PSR = P_{eng} / P_{req}$ is defined to quantify the positive power flows in the powertrain, where P_{eng} is the engine power and P_{req} is the power request from the driver. Four positive-power operating modes are defined: motor-only ($PSR = 0$), engine-only ($PSR = 1$), power-assist ($0 < PSR < 1$), and recharging mode ($PSR > 1$). The optimal (DP) behavior uses the motor-only mode in the low power-demand region at vehicle launch. When the wheel speed is above 6 rad/s, a simple rule is found by plotting the optimal PSR versus the power request over the transmission input speed, which is equivalent to torque demand at the torque converter output shaft (see Figure 13). The figure shows the optimal policy uses the recharging mode ($PSR > 1$) in the low torque region, the engine-only mode in the middle torque region, and the power-assist mode in the high torque region. This can be explained by examining a weighted Brake Specific Fuel Consumption and Emissions Production (BSFCEP) of the engine.

$$BSFCEP = \frac{W_f + \mu \cdot W_{NOx} + \upsilon \cdot W_{PM}}{P_{eng}} \quad (17)$$

The contour of engine BSFCEP map for $\mu = 40$ and $\upsilon = 800$ is shown in the Figure 14. It can be seen that the best BSFCEP region occurs at low torque levels. In order to move the engine operating points towards a better BSFCEP region, the engine recharges the battery at low load, and the motor is used to assist the engine at high load. In order to extract an implementable rule, a least-square curve fit is used to approximate the optimal PSR, shown as the solid line in Figure 13.

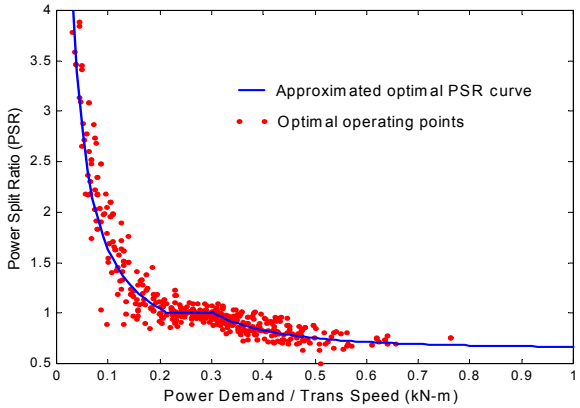

Figure 13: DP power split behaviour (UDDSHDV cycle)

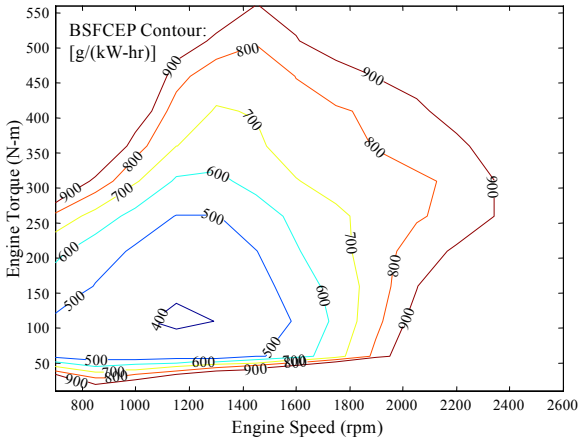

Figure 14: BSFCEP map in g/kWhr ($\mu = 40$ and $\upsilon = 800$)

C. *Charge-Sustaining Strategy*

The Power Split Control scheme described above does not maintain the battery SOC within desired operating range. An additional rule should be developed to prevent the battery from depleting or overcharging. The strategy for regulating the SOC still needs to be obtained in an approximately optimal manner in order to satisfy the overall goal: minimize fuel consumption and emissions. The DP procedure is repeated again with the regenerative braking function turned

off. In other words, no "free" energy from the regenerative braking is available to recharge the battery. After the optimization, the curve-fit optimal PSR result is computed, and compared with the result with regenerative braking. Figure 15 shows the recharging part is more important without regenerative braking. This is because increasing the engine power can move the engine's operation to the best BSFCEP region; the excess energy is stored for later use by the motor during high power demand. On the other hand, with the regenerative energy, the electric motor can act more aggressively to share the load with the engine since running the engine at high power is unfavorable for fuel economy and emissions. As a result, knowing the amount of the regenerative braking energy the vehicle will capture in future driving is the key to achieving the best fuel and emissions reduction while maintaining the battery SOC level. However, estimating the future amount of regenerative energy is not easy since future driving conditions are usually unknown. An alternative is to adjust the control strategy as a function of the battery SOC. For example, more aggressive spending of battery energy can be used when SOC is high and more conservative rules can be used when SOC is low. These adaptive PSR rules can be learned from DP results by specifying different initial SOC points.

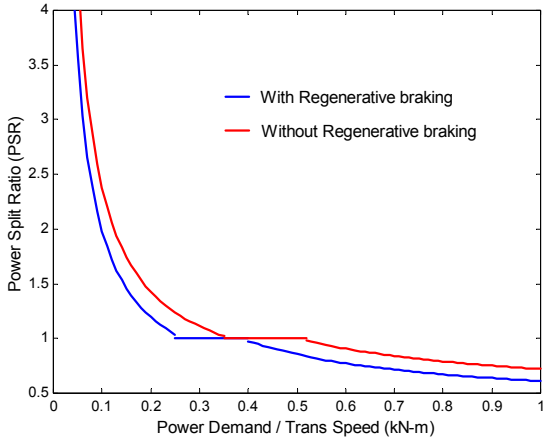

Figure 15: Optimal PSR rules comparison

D. Fuel Economy and Emissions Evaluation

After incorporating all the changes outlined in the previous sections, the improved rule-based controller is evaluated using several different driving cycles. In addition to the original cycle (UDDSHDV), the new rule-based controller is evaluated on three other driving cycles (suburban, interstate, and city) to test its robustness. The results are shown in Tables 5-8. It can be seen that depending on the nature of the driving cycles, the new rule-based control system may not improve all three categories of performance, and in certain cases did slightly worse. However, if the combined fuel/emission performance is considered (the "performance measure"), the new rule-based controller is always significantly better than the original, intuition-motivated rule-based control law.

Table 5: Results over the UDDSHDV cycle

	FE (mi/gal)	Nox (g/mi)	PM (g/mi)	Performance Measure *	
				g/mi	Improvement
Prelim. Rule-Based	13.16	5.740	0.458	840.63	0 %
New Rule-Based	12.82	4.87	0.44	793.16	5.65 %
DP (FE & Emiss.)	13.24	4.64	0.40	739.56	12.02%

Performance Measure: $fuel + 40 \cdot NOx + 800 \cdot PM$ (g/mi)

Table 6: Results over the WVUSUB cycle

	FE (mi/gal)	Nox (g/mi)	PM (g/mi)	Performance Measure *	
				g/mi	Improvement
Prelim. Rule-Based	15.31	4.43	0.36	671.23	0 %
New Rule-Based	14.61	3.02	0.30	582.18	13.27 %
DP (FE & Emiss.)	15.41	2.78	0.26	526.67	21.54 %

Table 7: Results over the WVUINTER cycle

	FE (mi/gal)	NOx (g/mi)	PM (g/mi)	Performance Measure*	
				g/mi	Improvement
Prelim. Rule-Based	12.84	7.29	0.51	948.83	12.84
New Rule-Based	12.72	6.31	0.49	896.00	12.72
DP (FE & Emiss.)	12.97	6.17	0.44	847.67	12.97

Table 8: Results over the WVUCITY cycle

	FE (mi/gal)	Nox (g/mi)	PM (g/mi)	Performance Measure	
				g/mi	Improvement
Prelim. Rule-Based	16.18	3.87	0.33	621.22	16.18
New Rule-Based	15.09	2.49	0.23	494.12	15.09
DP (FE & Emiss.)	16.63	2.04	0.16	403.58	16.63

VI. CONCLUSIONS

Designing the power management strategy for HEV by extracting rules from the Dynamic Programming results has the clear advantage of being near-optimal, accommodating multiple objectives, and systematic. Depending on the overall objective, one can easily develop power management laws that emphasize fuel economy, and/or emissions. By analyzing the DP results, an improved rule-based control strategy was developed. The extracted rules were found to be robust, and do not exhibit significant cycle-beating trait. This is evident by the fact that the rules based on one cycle work extremely well for several never-seen driving cycles. The improved rule-based control law, even given its simple structure, reduces its performance gap to the theoretically optimal (DP) results by 50-70%.

REFERENCES

[1] B. M. Baumann, et al., "Mechatronic Design and Control of Hybrid Electric Vehicles," IEEE/ASME Transactions on Mechatronics, vol. 5 no. 1, pp. 58-72, 2000

[2] S. D. Farrall and R. P. Jones, "Energy Management in an Automotive Electric/Heat Engine Hybrid Powertrain Using Fuzzy Decision Making,"

Proceedings of the 1993 International Symposium on Intelligent Control, Chicago, IL, 1993.
[3] C. Kim, E. NamGoong, and S. Lee, “Fuel Economy Optimization for Parallel Hybrid Vehicles with CVT,” SAE Paper No. 1999-01-1148.
[4] G. Paganelli, G. Ercole, A. Brahma, Y. Guezennec, and G. Rizzoni, “A General Formulation for the Instantaneous Control of the Power Split in Charge-Sustaining Hybrid Electric Vehicles.” Proceedings of 5th Int’l Symposium on Advanced Vehicle Control, Ann Arbor, MI, 2000.
[5] V.H. Johnson, K. B. Wipke, and D.J. Rausen, “HEV Control Strategy for Real-Time Optimization of Fuel Economy and Emissions,” SAE Paper No. 2000-01-1543, April 2000.
[6] A. Brahma, Y. Guezennec, and G. Rizzoni, “Dynamic Optimization of Mechanical Electrical Power Flow in Parallel Hybrid Electric Vehicles,” Proceedings of 5th Int’l Symposium on Advanced Vehicle Control, Ann Arbor, MI, 2000.
[7] U. Zoelch and D. Schroeder, “Dynamic Optimization Method for Design and Rating of the Components of a Hybrid Vehicle,” International Journal of Vehicle Design, vol. 19, no. 1, pp. 1-13, 1998.
[8] C.-C. Lin, J. Kang, J. W. Grizzle, and H. Peng, “Energy Management Strategy for a Parallel Hybrid Electric Truck,” Proceedings of the 2001 American Control Conference, Arlington, VA, June, 2001, pp. 2878-2883.
[9] D.N. Assanis, Z. S. Filipi, S. Gravante, D. Grohnke, X. Gui, L. S. Louca, G. D. Rideout, J. L. Stein, and Y. Wang, “Validation and Use of SIMULINK Integrated, High Fidelity, Engine-In-Vehicle Simulation of the International Class VI Truck,” SAE Paper No. 2000-01-0288, 2000.
[10] C.-C. Lin, Z. S. Filipi, Y. Wang, L. S. Louca, H. Peng, D. N. Assanis, and J. L. Stein, “Integrated, Feed-Forward Hybrid Electric Vehicle Simulation in SIMULINK and its Use for Power Management Studies”, SAE Paper No. 2001-01-1334, 2001.
[11] P. D. Bowles, “Modeling and Energy Management for a Parallel Hybrid Electric Vehicle (PHEV) with Continuously Variable Transmission (CVT),” MS thesis, University of Michigan, Ann Arbor, MI, 1999
[12] D. P. Bertsekas, Dynamic Programming and Optimal Control, Athena Scientific, 1995
[13] J. Kang, I. Kolmanovsky and J. W. Grizzle, “Dynamic Optimization of Lean Burn Engine Aftertreatment,” ASME J. Dynamic Systems Measurement and Controls, Vol. 123, No. 2, pp. 153-160, Jun. 2001.
[14] H. D. Lee, S. K. Sul, H. S. Cho, and J. M. Lee, “Advanced Gear Shifting and Clutching Strategy for Parallel Hybrid Vehicle with Automated Manual Transmission,” Proceedings of the IEEE Industry Applications, 1998.
[15] P. Soltic and L. Guzzella, "Optimum SI Engine Based Powertrain Systems for Lightweight Passenger Cars," SAE Paper No. 2000-01-0827, 2000
[16] Society of Automotive Engineers, Hybrid-Electric Vehicle test Procedure Task Force, “SAE J1711, Recommended Practice for Measuring Exhaust Emissions and Fuel Economy of Hybrid-Electric Vehicles,” 1998.
[17] D. L. Mckain, N. N. Clark, T. H. Balon, P. J. Moynihan, P. J. Lynch, and T. C. Webb, "Characterization of Emissions from Hybrid-Electric and Conventional Transit Buses," SAE Paper 2000-01-2011, 2000
[18] National Renewable Energy Laboratory, “ADVISOR 3.2 Documentation,” http://www.ctts.nrel.gov/analysis/ , 2001.
[19] I. Kolmanovsky, M. Nieuwstadt, and J. Sun, “Optimization of Complex Powertrain Systems for Fuel Economy and Emissions,” Proceedings of the 1999 IEEE International Conference on Control Applications, Hawaii, 1999.

Chan-Chiao Lin received the B.S. degree in power mechanical engineering from the National Tsing Hua University, Taiwan in 1995, and the M.S. degree from the National Taiwan University, Taiwan in 1997. He is currently a Ph.D. candidate in mechanical engineering at the University of Michigan, Ann Arbor. He receives the University of Michigan Rackham Fellowship in 2003. His research interests are modeling and control of hybrid vehicles.

Huei Peng received his Ph.D. in Mechanical Engineering from the University of California, Berkeley in 1992. He is currently an Associate Professor in the Department of Mechanical Engineering, University of Michigan, Ann Arbor. His research interests include adaptive control and optimal control, with emphasis on their applications to vehicular and transportation systems. He has been an active member of SAE and the ASME Dynamic System and Control Division. He has served as the chair of the ASME DSCD Transportation Panel from 1995 to 1997. He is currently an Associate Editor for the IEEE/ASME Transactions on Mechatronics. He received the National Science Foundation (NSF) Career award in 1998.

Jessy W. Grizzle received the Ph.D. in electrical engineering from The University of Texas at Austin in 1983. Since September 1987, he has been with The University of Michigan, Ann Arbor, where he is a Professor of Electrical Engineering and Computer Science. His research interests lie in the theory and practice of nonlinear control. He has been a consultant in the automotive industry since 1986, where he jointly holds fourteen patents dealing with emissions reduction through improved control system design. Professor Grizzle is a past Associate Editor of the Transactions on Automatic Control and Systems & Control Letters, and is currently an Associate Editor for Automatica. He served as Publications Chairman for the 1989 CDC, from 1997 through 1999 served on the Control Systems Society's Board of Governors, and was Chair of the IEEE Control Systems Society Fellows Solicitation Committee from 2000 through 2003. He was a NATO Postdoctoral Fellow from January to December 1984; he received a Presidential Young Investigator Award in 1987, the Paper of the Year Award from the IEEE Vehicular Technology Society in 1993, the University of Michigan's Henry Russell Award for outstanding research in 1993, a College of Engineering Teaching Award, also in 1993, was elected a Fellow of the IEEE in 1997, and received the 2002 George S. Axelby Award (for the best paper published in the IEEE Transactions on Automatic Control during the years 2000 and 2001).

Jun-Mo Kang received the B.E.E. degree in Electrical Engineering from the Korea University in 1993, and the M.S. and Ph.D. degrees in electrical engineering and computer science from the University of Michigan, Ann Arbor, in 1997 and 2000. His research interests are in control and modeling of advanced technology engines and optimization of dynamic systems. He is currently a Senior Research Engineer at General Motors R&D in Warren, MI.